Surface Plasmon Resonance and Nuclear Magnetic Resonance Studies of ABAD−Aβ Interaction†

Yilin Yan,‡ Yangzhong Liu,‡,§ Mirco Sorci,|| Georges Belfort,|| Joyce W. Lustbader,⊥ Shirley ShiDu Yan,@ and Chunyu Wang*,‡

Department of Biology, Center for Biotechnology and Interdisciplinary Studies, Rensselaer Polytechnic Institute, Troy, New York 12180, Department of Chemical and Biological Engineering, Center for Biotechnology and Interdisciplinary Studies, Rensselaer Polytechnic Institute, Troy, New York 12180, Center for Reproductive Sciences and Department of Obstetrics and Gynecology, College of Physicians and Surgeons, Columbia University, 630 West 168th Street, New York, New York 10032, and Department of Pathology and Surgery, College of Physicians and Surgeons, Columbia University, 630 West 168th Street, New York, New York 10032

Received June 29, 2006; Revised Manuscript Received December 12, 2006

ABSTRACT: Aβ binding alcohol dehydrogenase (ABAD) is an NAD-dependent mitochondrial dehydrogenase. The binding between ABAD and Aβ is likely a direct link between Aβ and mitochondrial toxicity in Alzheimer's disease. In this study, surface plasmon resonance (SPR) was employed to determine the temperature dependence of the affinity of the ABAD−Aβ interaction. A van't Hoff analysis revealed that the ABAD−Aβ association is driven by a favorable entropic change ($\Delta S = 300 \pm 30$ J mol^{-1} K^{-1}) which overcomes an unfavorable enthalpy change ($\Delta H = 49 \pm 7$ kJ/mol). Therefore, hydrophobic interactions and changes in protein dynamics are the dominant driving forces of the ABAD−Aβ interaction. This is the first dissection of the entropic and enthalpic contribution to the energetics of a protein−protein interaction involving Aβ. SPR confirmed the conformational changes in the ABAD−Aβ complex after Aβ binding, consistent with differences seen in the crystal structures of free ABAD and the ABAD−Aβ complex. Saturation transfer difference (STD) NMR experiments directly and unambiguously demonstrated the inhibitory effect of Aβ on the ABAD−NAD interaction. Conversely, NAD inhibits the Aβ−ABAD interaction. Binding of Aβ and binding of NAD to ABAD are likely mutually exclusive. Thus, Aβ binding induces conformational and subsequently functional changes in ABAD, which may have a role in the mechanism of Aβ toxicity in Alzheimer's disease.

Aβ is believed to be the primary influence in causing Alzheimer's disease (AD).[1] The amyloid hypothesis proposes that Aβ triggers a cascade of pathological events which eventually lead to neuronal dysfunction, neuronal death, and dementia (*1*, *2*). However, the detailed molecular mechanisms of Aβ neuronal toxicity are still unclear (*1*, *3*). Aβ binding alcohol dehydrogenase (ABAD), a mitochondrial enzyme, links Aβ toxicity with mitochondrial oxidative stress through ABAD−Aβ interaction (*4*, *5*). ABAD−Aβ interaction likely plays an important role in the pathogenesis of Alzheimer's disease and thus represents a novel target for disease-modifying therapeutics for AD.

ABAD is a member of the short-chain dehydrogenase reductase family present in the mitochondria of neurons (*6*−*9*). Using NAD and/or NADH as its cofactor, ABAD catalyzes the reversible oxidation and/or reduction of alcohol groups in a wide range of substrates, including the ketone body (β-hydroxybutyrate), linear alcohols, branched fatty acids, steroids, and isoleucine catabolites, methyl-3-hydroxylbutyryl-CoA (MHB) (*10*, *11*). Overexpressing ABAD in COS cells in a medium where β-hydroxybutyrate is the only energy source showed protective function on cell viability and ATP content (*5*), suggesting the important role of ABAD in the cellular response to nutritional stress. In response to ischemic stress, transgenic mice overexpressing ABAD exhibited decreased neurological deficiency compared with the control mice (*5*). The neuronal protective function of

† C.W. gratefully acknowledges a new investigator award from the Alzheimer's Association. C.W. is also funded by the James D.Watson Young Investigator program of NYSTAR of New York State. S.S.Y. is supported by NIH Grants AG16736, P01AG17490, and P50AG08702 and the Alzheimer's Association.

* To whom correspondence should be addressed. E-mail: wangc5@rpi.edu. Phone: (518) 276-3497. Fax: (518) 276-4207.

‡ Department of Biology, Center for Biotechnology and Interdisciplinary Studies, Rensselaer Polytechnic Institute.

§ Present address: Department of Chemistry, University of Science and Technology of China (USTC), Hefei, Anhui, PR China 230026.

|| Department of Chemical and Biological Engineering, Center for Biotechnology and Interdisciplinary Studies, Rensselaer Polytechnic Institute.

⊥ Center for Reproductive Sciences and Department of Obstetrics and Gynecology, College of Physicians and Surgeons, Columbia University.

@ Department of Pathology and Surgery, College of Physicians and Surgeons, Columbia University.

[1] Abbreviations: SPR, surface plasmon resonance; NMR, nuclear magnetic resonance; ABAD, Aβ binding alcohol dehydrogenase; AD, Alzheimer's disease; STD, saturation transfer difference; NAD, nicotinamide adenine dinucleotide; APP, amyloid precursor protein; Aβ, amyloid β peptide; ADDL, Aβ-derived diffusive ligand; RAGE, receptor for advanced glycation end products; DP, decoy peptide; ROS, reactive oxygen species; MHB, 2-methyl-3-hydroxylbutyrate; LB, Luria-Bertini medium; MPTP, 1-methyl-4-phenyl-1,2,3,6-tetrahydropyridine; AFM, atomic force microscopy.

10.1021/bi061314n CCC: $37.00
Published on Web 01/25/2007

ABAD was also shown by overexpressing ABAD in the murine 1-methyl-4-phenyl-1,2,3,6-tetrahydropyridine (MPTP) model of Parkinsonism with impaired mitochondrial respiration (*12*). ABAD deficiency was initially studied with the inactivation of the ABAD homologue in *Drosophila*, termed *scully*, which leads to developmental abnormalities in mitochondria and a lethal phenotype (*13*). Clinical cases of ABAD deficiency were reported recently (*11*, *14*, *15*). Patients with mutant ABAD are characterized by an increased level of urinary MHB and the absence of MHB dehydrogenase activity. Neurological symptoms include psychomotor retardation and progressive infantile neurodegeneration. Thus, ABAD plays important roles in a cellular response to stress, the energy metabolism of mitochondria, and the breakdown of isoleucines in normal neurons (*16*).

In Alzheimer's disease, ABAD−Aβ interaction links Aβ toxicity with mitochondrial dysfunction via mitochondrial oxidative stress (*4*). An increased expression level of ABAD was observed in inferior temporal lobe gyrus and hippocampus in AD brains (*4*, *5*). ABAD and Aβ were shown to be colocalized in mitochondria in AD brains by confocal microscopy and electron microscopy (*4*). Aβ most likely enters the mitochondria through ER-to-mitochondrion transfer (*17*). Although both γ-secretase activity and APP are present on the mitochondrial membrane (*18*, *19*), the arrested mode of insertion of APP into the mitochondrial membrane, with the entire Aβ sequence and γ-secretase site exposed on the cytoplasmic side, may preclude cleavage by γ-secretase (*18*, *19*). ABAD was the only human protein found to interact with Aβ in a yeast two-hybrid screening (*9*), and this interaction was shown to inhibit the enzymatic activity of ABAD toward multiple substrates (*10*). Double-transgenic mice (Tg mAPP/ABAD) overexpressing ABAD and mAPP (APP with V717F, K670M, and N671L mutations), which provides an Aβ-rich environment, were generated to study the role of ABAD−Aβ interaction in mitochondrial oxidative stress and neurodegenerative diseases. These double-transgenic mice exhibited increased mitochondrial stress, apoptosis of neurons, and an accelerated decline in learning and memory compared with single-transgenic Tg mAPP mice, Tg mABAD mice, and non-Tg mice (*4*, *20*). In neurons from the Tg mAPP/ABAD mice, higher levels of free radical-induced stress based on oxidation of 2′,7′-dichlorofluorescein were observed in comparison with neurons from other genotypes (*4*). A 29-amino acid peptide, ABAD decoy peptide (DP) which shares the same amino acid sequence with the L_D loop (residues C91−D119) in ABAD, inhibits ABAD−Aβ interaction. Mutagenesis and inhibition studies have established that the L_D loop plays a critical role in Aβ binding (*4*). When DP was added into cultured neurons from Tg mAPP/ABAD mice, the oxidative stress was inhibited (*4*). These data strongly suggest Aβ executes its cytotoxicity through the interaction with ABAD (*16*, *21*−*23*) in these transgenic mice. In an Aβ-rich environment, ABAD binds to Aβ and becomes dysfunctional. The ABAD−Aβ complex may block essential metabolic steps in mitochondria, leading to reduced cytochrome *c* activity, generation and leakage of ROS from the mitochondria, the activation of a programmed cell death pathway, and ultimately loss of viability for neurons (*20*). Detailed understanding of this interaction is relevant to structure-based AD therapies in at least two ways. First, a drug can be designed to disrupt Aβ−ABAD interaction. Second, a high-affinity Aβ ligand may be designed to inhibit the formation of Aβ oligomers or fibrils and to inhibit the interaction between Aβ and other Aβ target proteins.

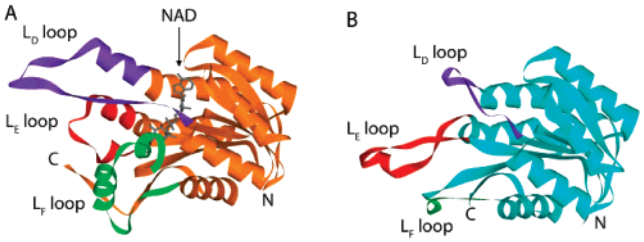

FIGURE 1: Structures of human ABAD in complex with NAD (A) and Aβ (B). ABAD has a typical, dehydrogenase Rossman fold. The L_D, L_E, and L_F loops, which undergo large changes upon Aβ binding, are colored purple, red, and green, respectively, and NAD is colored gray. Aβ binds to ABAD and alters the conformation and dynamics of the L_D, L_E, and L_F loops. NAD was not observed in the crystal structure of the ABAD−Aβ complex even though the crystallization buffer included NAD.

Several crystal structures of ABAD have been determined (*4*, *8*, *24*), and ABAD has a typical dehydrogenase Rossman fold for dinucleotide binding (Figure 1A). The NAD molecule has numerous interactions with residues in the L_D, L_E, and L_F loops. NAD interacts with the catalytic triad (S155, Y168, and K172) in the L_E loop through hydrogen bonding with K172 and Y168, and through hydrophobic interaction with S155. The structural basis of inhibition of Aβ of ABAD enzyme activity was suggested by the recently determined crystal structure of the ABAD−Aβ complex. In this complex, the L_D, L_E, and L_F loops are deformed and have decreased electron density, leading to prominent distortions of the NAD binding pocket (Figure 1B) (*4*). No electron density was observed for NAD in the ABAD−Aβ complex which was crystallized with NAD (Figure 1B), suggesting NAD cannot bind to the ABAD−Aβ complex. The lack of NAD density can nonetheless also result from NAD dynamics or static disorder. Therefore, it is still unclear whether NAD can bind to the Aβ−ABAD complex. The critical interface between ABAD and Aβ was not observed due to the lack of electron density for Aβ and the L_D loop. Thus, the biophysical basis of the ABAD−Aβ interaction is still poorly understood.

To probe the driving forces of the ABAD−Aβ interaction, surface plasmon resonance (SPR) was employed to determine the entropy change and the enthalpy change of the ABAD−Aβ interaction. SPR data also confirmed the presence of conformational changes in the ABAD−Aβ complex subsequent to Aβ binding. Saturation transfer difference (STD) experiments were applied to directly demonstrate that Aβ inhibits the NAD−ABAD interaction. Conversely, SPR revealed that large amounts of NAD inhibit the ABAD−Aβ interaction.

MATERIALS AND METHODS

ABAD Purification. Escherichia coli strain BL21(DE3) transformed with pGE5-encoding human ABAD was grown in Luria-Bertini medium (LB) (*10*). Cells were induced with 0.5 mM isopropyl 1-thio-β-D-galactopyranoside (IPTG) at an A_{600} of ~0.6 and harvested by centrifugation at 4000 rpm after induction for 4 h. The cell pellet was resuspended in 40 mL (per 2 L of bacterial culture) of 25 mM MES (pH

6.0), 100 mM NaCl, 10 mM DTT, and 0.5 mM PMSF. Extracts of the soluble protein were subjected to cation exchange FPLC on an SP-Sepharose FF column (GE Amersham Biosciences) followed by gel filtration on a Superdex 200 column. The SP column was equilibrated with 25 mM MES and 5 mM DTT (pH 6.0) and eluted with an ascending linear salt gradient (from 0.0 to 0.4 M NaCl). ABAD elutes at ~0.15 M NaCl, and the ABAD-rich fractions were collected and concentrated by ultrafiltration to 20 mg/mL and loaded onto a Superdex 200 column (2 mL was applied to the column for each run) equilibrated with 25 mM MES (pH 6.0), 100 mM NaCl, and 10 mM DTT. Peak fractions from the Superdex 200 column were collected and verified by SDS−PAGE and an enzyme activity assay.

SPR Study of ABAD−Aβ Interaction. SPR has been employed in studying Aβ aggregation and Aβ−ApoE and Aβ−membrane interaction (*25*). Aβ40 was obtained from rPeptide (www.rpeptide.com, catalog no. A-1156-2). SPR studies were performed on a BIAcore 3000 system (BIAcore AB, Uppsala, Sweden). Aβ (500 μg/mL) in 10 mM sodium acetate (pH 5.0) (*26*) was immobilized using the standard amino coupling on a research-grade CM5 sensor chip (BIAcore) (*27*). Due to the large size of the ABAD tetramer (108 kDa), pronounced RU changes were observed when free ABAD (the analyte) binds Aβ (the ligand) immobilized on the chip. The Tris running buffer contained 50 mM Tris-HCl (pH 7.5) and 150 mM sodium chloride. The flow rate was 40 μL/min to minimize the mass transfer effect. Four different concentrations of ABAD (3.75, 1.25, 0.42, and 0.14 μM) were injected during the 90 s association phase, and the chip surface was exposed to running buffer for 120 s to monitor the dissociation phase. The chip surface was regenerated by the injection of 40 μL of regeneration buffer [4 M guanidine-HCl in 10 mM Tris-HCl (pH 8.0)] (*26*). Data from a control cell without Aβ immobilization were subtracted from raw data. A running buffer injection using the same injection method was always applied before each injection and subtracted for double reference. The binding curves were analyzed with the global fitting model using BIAevaluation version 4.0.1 (BIAcore AB). Immobilization of Aβ in SPR experiments may alter the affinity or kinetics of the Aβ−ABAD interaction; however, the dextran layer where Aβ was immobilized retains many of the rotational properties of the macromolecule and some degree of translational diffusion freedom (*28*). Myszka et al. have demonstrated that carefully executed SPR measurements generate affinity data in excellent agreement with data obtained from solution-based methods in two model systems (*29*, *30*).

Immobilization of Aβ monomers, prepared by NaOH treatment (*31*), did not show binding to ABAD in SPR experiments. No binding was observed in the NMR titration of ABAD into Aβ monomers (data not shown). Therefore, ABAD does not bind to Aβ monomers. The Aβ used for immobilization onto the sensor chip was composed of oligomers, as demonstrated by atomic force microscopy (AFM, Figure 2A,B). 6E10 antibody, which recognizes all species of Aβ, blocked the binding between Aβ and ABAD in SPR experiments (data not shown), while A11, a nonspecific antibody against oligomers of many proteins (*32*), did not block binding. Therefore, ABAD binds to Aβ oligomers not recognized by A11 antibody. A large cavity observed in the crystal structure of the ABAD−Aβ complex which can easily accommodate Aβ oligomer also suggested that ABAD binds to the oligomeric form of Aβ (*4*, *16*). Aβ oligomers are mixtures of species with different sizes; therefore, the stoichiometry of the interaction between Aβ and ABAD cannot be determined at this stage. Indeed, because of this difficulty, no stoichiometry has been determined in published SPR studies of Aβ interactions (*33*−*35*). However, the correct measurement of affinity using SPR is not dependent on the knowledge of stoichiometry.

Atomic Force Microscopy (AFM) of the Aβ40 Solution Used for SPR. Images of Aβ40 were obtained with an MFP-3D atomic force microscope (Asylum Research, Santa Barbara, CA) and standard Si cantilevers (AC240TS, Olympus America Inc., Center Valley, PA). The Aβ solution used for immobilization onto the SPR sensor chip was diluted to 4 μM and placed on a mica surface for adsorption for 5 min. Nonadsorbed protein was washed away with water. Three-dimensional measurements at the nanometer scale were collected in air using the tapping mode technique of AFM and analyzed with IGOR Pro 5 (WaveMetrics, Inc., Lake Oswego, OR).

Conformational Change Determined by SPR. To test the effect of association time on the molecular interaction between ABAD and Aβ, different volumes of 3 μM ABAD samples (20, 60, 120, and 240 μL) were injected onto the Aβ-immobilized sensor chip at a flow rate of 40 μL/min. At the end of the each injection, running buffer was passed over the sensor surface for 26 min to observe the dissociation rate.

van't Hoff Analysis. To determine the enthalpy change and the entropy change of the ABAD−Aβ interaction, the equilibrium dissociation constants provided by the ratios of the kinetic rate constants were measured at six different temperatures, 10, 15, 20, 25, 30, and 35 °C. van't Hoff analysis was carried out assuming ΔH and ΔS of the ABAD−Aβ interaction vary negligibly with temperature, using the following equation:

$$\ln K_D = \Delta H_{\text{van't Hoff}}/RT - \Delta S/R$$

where R is the universal gas constant (8.31 J mol^{-1} K^{-1}) and T is the absolute temperature in kelvin.

STD Study of Aβ Inhibition of ABAD−NAD Interaction. STD is an elegant NMR tool for studying the interaction between protein and small molecules in the solution state (*36*, *37*). STD experiments were carried out on a Bruker 600 MHz spectrometer at 298 K equipped with a cryoprobe according to the method of Meyer and Mayer (*36*). STD−NMR spectra were recorded with 512 scans, and selective saturation of protein resonances at −1 ppm was achieved using a 2.049 s strain of 50 ms Gaussian pulses with a 32 Hz field, separated by a delay of 1 ms. No NAD resonance is present near −1 ppm. Due to spin diffusion in a large molecule, irradiation at −1 ppm quickly results in selective saturation of all proton signals in the 108 kDa ABAD tetramer. The NMR sample contains 200 μM NAD and 8.3 μM ABAD in MES buffer [25 mM MES and 100 mM NaCl (pH 6.0)]. Control experiments using the free ligands (NAD only) and a control protein (NAD and an engineered intein) were performed under the same experimental conditions, and

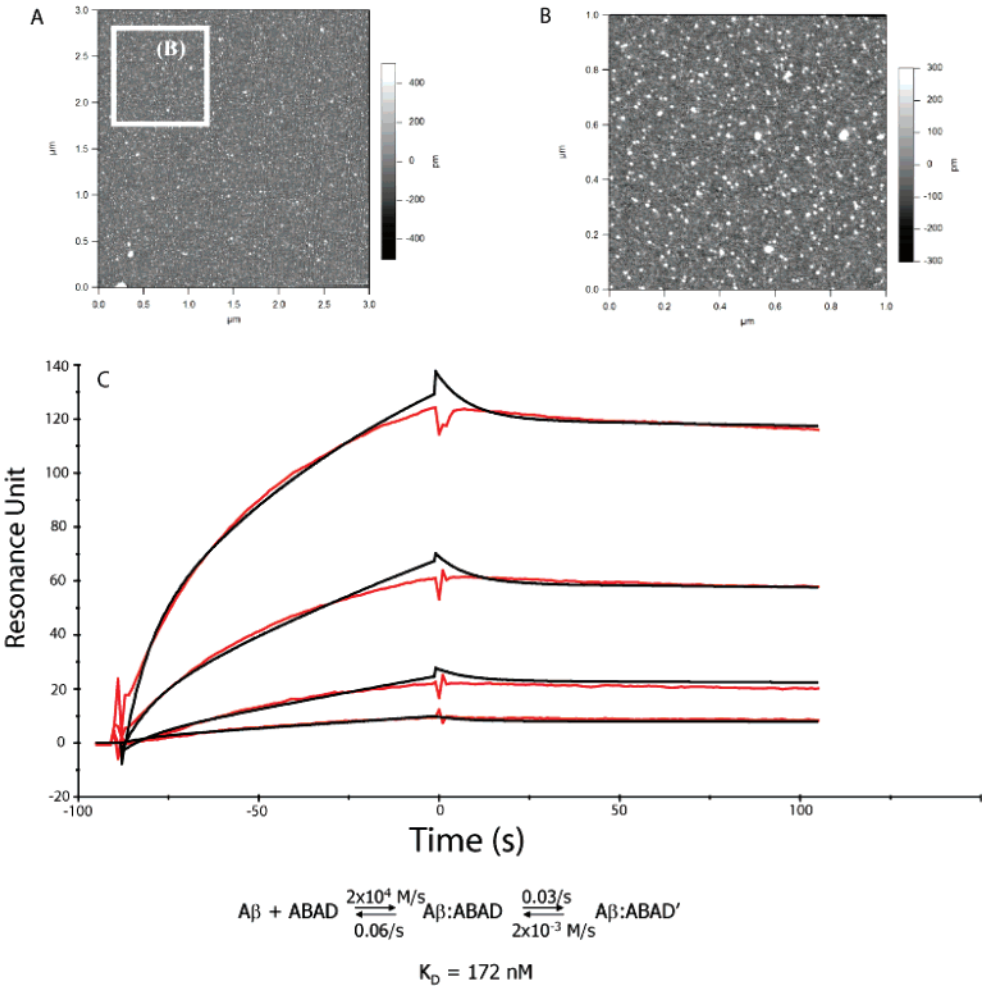

FIGURE 2: AFM images of Aβ and typical SPR data of the ABAD−Aβ interaction. (A) AFM images of Aβ used for immobilization onto the SPR sensor chips. The Aβ oligomers were mostly homogeneous with an average diameter of 15−20 nm. A few larger aggregates were present, but no fibrils could be observed. (B) Magnification of a selected AFM area of panel A. (C) Typical sensorgram of ABAD−Aβ interaction. Different concentrations of ABAD (11, 3.7, 1.2, 0.4, and 0.14 μM) were injected in the 90 s association time, and the dissociation time was 120 s. Globally fit data (red lines) using a conformational change model were overlaid with experimental data (black lines). There are two steps in the ABAD−Aβ interaction: Aβ and ABAD associate, and then a conformational change slowly occurs, resulting in ABAD′ with altered structure. The dissociation constant (K_D) was determined to be 172 nM at 25 °C.

no STD signal was observed. The inhibitory effect of Aβ on NAD−ABAD binding was probed by the changes in STD intensity with varying amounts of Aβ in the NMR sample, 0, 30, and 40 μM.

NAD resonances were assigned by two-dimensional TOCSY and two-dimensional NOESY spectra. In the aromatic region of the NMR spectra of free NAD, the triplet splitting established the assignment of N-H5 at 8.2 ppm. N-H5 shows two distinct intrabase NOEs to N-H4 (8.8 ppm) and N-H6 (9.1 ppm). The assignment of N-H1′ at 6.1 ppm was determined by two NOE peaks, one to N-H2 and the other to N-H6 at 9.3 and 9.1 ppm, respectively. A-H1′ was identified by its characteristic chemical shift at 6.0 ppm and an NOE peak to H8 at 8.4 ppm. The assignment process described above left the peak at 8.1 ppm in the aromatic region as the only candidate for A-H2.

NAD Inhibition of the Aβ−ABAD Interaction. New running buffers with different concentrations of NAD (1, 10, 100, and 500 μM) were prepared by adding different amounts of NAD into the Tris running buffer described above. ABAD (5 μM) was preincubated in the new running buffers with different NAD concentrations for 5 min before injection. Samples were injected in KINJECT mode (60 μL) at a flow rate of 40 μL/min. The chip surface was then exposed to the same running buffer containing NAD for 120 s to observe dissociation.

RESULTS

Conformational Changes in ABAD Caused by Aβ Association. SPR was employed in studying the kinetics and thermodynamics of ABAD−Aβ interaction. As shown in panels A and B of Figure 2, the Aβ solution used for immobilization contained Aβ oligomers. Therefore, the SPR sensor chip was immobilized with Aβ oligomers instead of Aβ fibrils, and our SPR data reported the thermodynamics of the interaction between Aβ oligomers and ABAD. The stability of Aβ oligomers was confirmed by obtaining consistent SPR results after many cycles of regeneration over the course of a week's time. A typical series of sensograms are shown in Figure 2C with data acquired with the injection of 0.14, 0.4, 1.2, 3.7, and 11 μM ABAD in the association phase. However, the resonance unit (RU) of this binding reaction did not reach plateau even with 30 min of association time (data not shown). The binding reactions for a simple

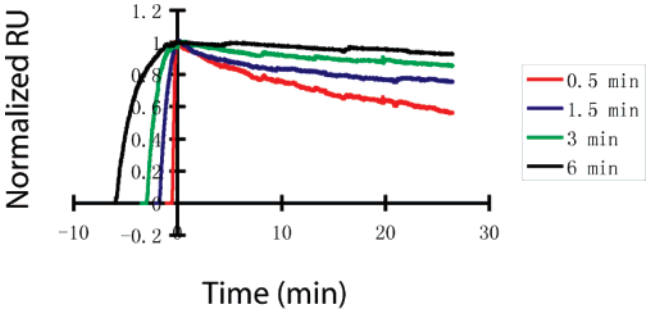

FIGURE 3: Various contact time experiment examining the ABAD−Aβ interaction. A 3 μM sample of ABAD was injected over the surface-immobilized Aβ(1−40) for 0.5, 1.5, 3, and 6 min. Data were normalized by setting the response at the start of the dissociation phase to 1. The uniform scaling of each SPR curve preserves the slope in the dissociation phase (*40*). The longer association time caused slower dissociation, indicating the presence of a conformational change in the ABAD−Aβ interaction.

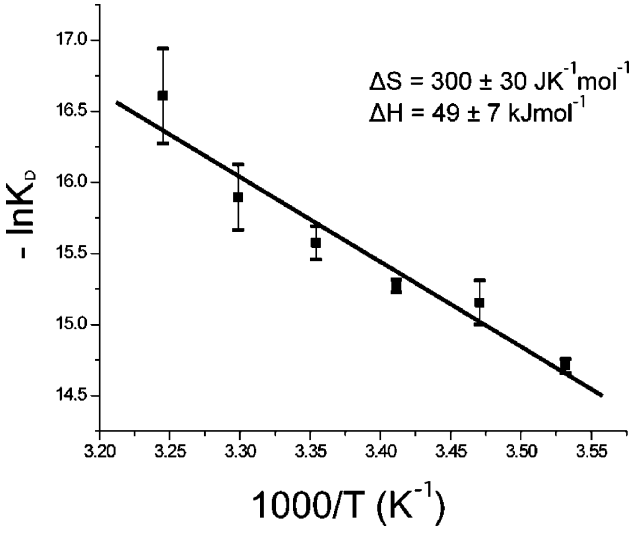

FIGURE 4: Enthalpy and entropy changes of ABAD−Aβ interaction from SPR. van't Hoff analysis of the ABAD−Aβ interaction at six different temperatures yielded a ΔH of 49 ± 7 kJ/mol and a ΔS of 300 ± 30 J mol^{-1} K^{-1}. This indicates ABAD−Aβ interaction is driven by favorable entropy change which overcomes the unfavorable enthalpy change.

bimolecular reaction would normally plateau once equilibrium was reached. Failure to plateau during the association phase suggested ABAD and/or Aβ may undergo conformational changes after ABAD−Aβ association.

To confirm such conformational changes, the dissociation rates with different association times were compared (Figure 3). For binding interactions without any conformational change, the dissociation rate should be independent of the length of the association phase. For a binding event accompanied by a slower conformational change, a longer association phase will result in conformational changes in more bimolecular complexes, leading to slower dissociation rates in the dissociation phase. This method for determining conformational change has been used by many SPR studies (*38*−*41*). ABAD was injected with different association times (0.5, 1.5, 3, and 6 min). For the better appreciation of differences in dissociation rates with different lengths of association time, the individual sensogram was scaled so that the RU at the beginning of dissociation phase was set to 1. Such scaling preserves the slope of the curve in the dissociation phase. This method for data presentation was first developed by Myszka et al. (*40*) and has been recently used by Munoz et al. (*39*). The normalized responses shown in Figure 3 indicate that the bound ABAD dissociates slower with longer association times (shallower slope of the RU curve), confirming that the ABAD−Aβ complex undergoes conformational changes while ABAD binds Aβ. This is consistent with the large conformational differences in ABAD observed between the crystal structures of the ABAD−Aβ complex and the Aβ-free ABAD (Figure 1) (*4*). Therefore, both our SPR data (Figures 2C and 3) and crystal structures of ABAD (Figure 1) indicated there are conformational changes upon formation of the ABAD−Aβ complex.

Affinity of ABAD−Aβ Interaction from SPR. Accordingly, a conformational change model was chosen to fit the SPR data. As shown in Figure 2C, ABAD−Aβ binding curves were well fit with the conformational change model to yield a dissociation constant (K_D) of 172 nM at 298 K. The affinity between Aβ and ABAD (60 ± 20 nM, at 35 °C) obtained by the conformational change model agreed well with the affinity measured by biochemical methods (K_D = 38 ± 5 nM, at 37 °C) (*4*). Although the concentration of Aβ in plasma and CSF is on the order of 0.1 nM (*42*), the local concentrations of Aβ might be much higher, e.g., in or near senile plaques, in neuronal mitochondria or in synapses where Aβ can be significantly enriched.

Entropy Change and Enthalpy Change of the ABAD−Aβ Interaction. To better understand the driving forces of ABAD−Aβ interaction, the temperature dependence of the ABAD−Aβ interaction was studied by SPR at six temperatures, ranging from 10 to 35 °C in 5 °C intervals (Figure 4). A least-squares linear fit (correlation coefficient R = 0.97) yields a $\Delta H_{\text{van't Hoff}}$ of 49 ± 7 kJ/mol from the slope and a ΔS of 300 ± 30 J mol^{-1} K^{-1} from the Y-axis intercept. Thus, the favorable ΔS overcomes the unfavorable ΔH and drives the association between ABAD and Aβ. The large positive ΔS suggests that hydrophobic interaction and an increase in protein dynamics play dominant roles in the ABAD−Aβ interaction. This is the first time that the entropic and enthalpic contributions have been dissected in any protein−protein interaction involving Aβ.

Aβ Inhibition of the ABAD−NAD Interaction. SPR cannot be utilized to study NAD−ABAD interaction because of the small size of NAD. Saturation transfer difference (STD) is an elegant solution NMR method for the direct observation of the binding between small molecules and large proteins (*36*). In an STD experiment, protein resonances are selectively saturated by long, weak RF irradiation in a narrow frequency region where no ligand resonances are present. Due to the large size of proteins, all the protein proton resonances are quickly saturated by efficient spin diffusion. When the ligand binds to the saturated protein, the saturation is transferred from the protein to the ligand resonances due to the proximity of ligand protons and protein protons at the interface. Because of the long T_1 of small molecules, the ligand resonances will remain saturated after dissociation from the protein. Therefore, if there is binding between protein and ligand, the signal intensity of the free ligand will be attenuated even when only the protein resonances are being saturated. When a difference NMR spectrum of the free ligand is taken between the NMR spectra with and

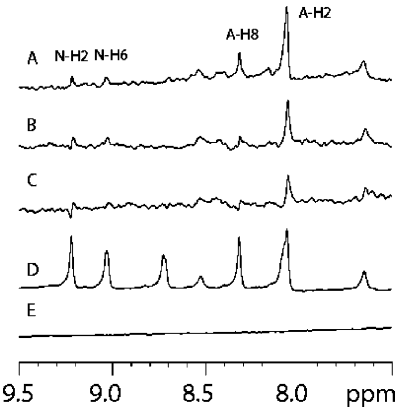

FIGURE 5: Aβ inhibition of the ABAD−NAD binding by STD NMR. (A) STD signals of NAD (200 μM NAD and 8.3 μM ABAD) without Aβ. STD demonstrated the binding of NAD with ABAD. The magnitudes of the STD signals decreased after addition of Aβ to 30 μM (B) and 40 μM (C), indicating Aβ inhibits the ABAD−NAD interaction. The one-dimensional spectrum of NAD with assignment (D) and the null STD spectrum of free NAD (E) are also shown.

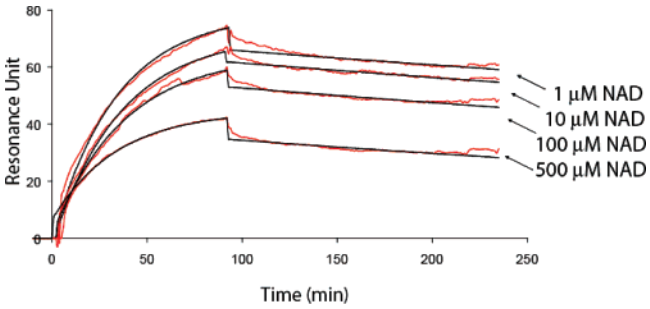

FIGURE 6: NAD inhibition of the ABAD−Aβ interaction by SPR. ABAD (5 μM) was preincubated with different concentrations of NAD. Fit data (red lines) were overlaid with experimental data (black lines). There was a progressive decrease in RU of ABAD−Aβ interaction with an increase in the concentration of NAD.

without the selective saturation of protein, ligand resonances responsible for protein binding are revealed. STD signals not only demonstrate binding between protein and ligand but also map the binding epitope of the ligand. STD has also been utilized to study competition in the binding of ligand to proteins (*37*).

To directly observe the effect of Aβ on the NAD−ABAD interaction in solution, the STD signal of NAD−ABAD binding was monitored in the presence of different concentrations of Aβ while the other conditions of the NMR sample were kept constant. Under such conditions, the STD signal strength is proportional to the concentration of NAD bound to ABAD. In the absence of Aβ (Figure 5A), STD signals indicate that protons N-H2, N-H6, A-H2, and A-H8 in NAD are in contact with ABAD, consistent with the crystal structure of the ABAD−NAD complex (*24*). As shown in panels B and C of Figure 5, increasing the concentration of Aβ progressively decreased the magnitude of the STD signal of NAD−ABAD binding. Therefore, less NAD bound to ABAD with an increase in the concentration of Aβ, demonstrating the inhibitory effect of Aβ on the interaction between NAD and ABAD.

NAD Inhibition of the ABAD−Aβ Interaction. To address the reverse question of whether NAD inhibits the ABAD−Aβ interaction, ABAD was injected for SPR binding experiments after preincubation with different concentrations of NAD (1, 10, 100, and 500 μM). As shown in Figure 6, the addition of NAD causes a progressive drop in RU in the binding of ABAD to Aβ. Thus, NAD also inhibits ABAD−Aβ binding. Together with the STD data, the NAD inhibition data obtained from SPR suggest that binding of Aβ to ABAD and binding of NAD to ABAD are mutually exclusive.

DISCUSSION

In this work, we demonstrate with SPR that the binding of Aβ to ABAD causes conformational changes in the ABAD−Aβ complex, consistent with findings from crystallographic studies (*4*). In addition, we directly and unequivocally demonstrate that Aβ inhibits NAD−ABAD binding in solution using STD, most likely as a result of the conformational changes. Loss of NAD was clearly shown with the decrease in the magnitude of STD signals with Aβ titration. By displacing the NAD molecule, Aβ should inhibit the enzymatic activity of ABAD toward all substrates, which was borne out in experiments with multiple substrates, including *S*-acetoacetyl-CoA, octanol, and 17β-estradiol (*10*). In addition, Aβ binding may inhibit ABAD enzymatic activity by displacing ABAD substrates, which remains to be clarified by additional experiments. Because of the important role of ABAD in mitochondrial energy metabolism and in amino acid catabolism, the loss of ABAD activity leads to mitochondrial dysfunction. The dysfunction of mitochondrial energy metabolism inhibits ATP production, impairs calcium buffering, and generates reactive oxygen species (ROS) (*43*−*45*). In Alzheimer's disease, impaired energy metabolism and oxidative damage occur in the early stage before Aβ deposition (*46*). Incubation of soluble Aβ42 with two kinds of cells (with mitochondrial DNA and without mitochondrial DNA) displayed decreased viability in cells with mitochondrial DNA but intact viability in cells without mitochondrial DNA (*47*). This strongly suggests functional mitochondria may be critical for cellular toxicity induced by soluble Aβ in cells in many cases. Aβ progressively accumulates in mitochondria (*17*) and interacts with ABAD, which induces the generation of free radicals and oxidative damage in AD.

In this study, we demonstrate that the ABAD−Aβ interaction has a positive entropy change and a positive enthalpy change. The enthalpy is a measure of the average potential energy of interaction between molecules, whereas the entropy is a measure of the disorder of the system. Because the free Aβ in solution is flexible (*31*, *48*), it will lose entropy subsequent to binding to ABAD, which is a large source of negative Δ*S*. Positive Δ*S* which overcomes the entropy loss associated with Aβ binding may have two sources: the increase in the dynamics of water (hydrophobic interaction) and the increase in the protein dynamics of ABAD. The large positive entropy change is most likely due to the release of ordered water from around the hydrophobic areas upon the burial of these surfaces during ABAD−Aβ association, which results in the increase of the dynamics of water (hydrophobic interaction). Mutagenesis and inhibition studies demonstrated that the L_D loop of ABAD is likely responsible for binding Aβ (*4*). Aβ20 displayed a similar binding affinity for ABAD compared with that of full-length Aβ, whereas Aβ(25−35) exhibited no binding affinity for ABAD, indicat-

ing that Aβ(1−20) mediates the ABAD−Aβ interaction (*4*). Via a comparison of the sequences of Aβ(1−20) and the L_D loop, the hydrophobic interaction between ABAD and Aβ likely occurs between the central hydrophobic cluster (CHC) of Aβ(17−20, LVFF) and hydrophobic residues in the L_D loop (Y101, and residues 92−97 with the AGIAVA sequence). The additional origin of positive ΔS may come from the increased dynamics in ABAD. In the crystal structure of the ABAD−Aβ complex, there is a loss of electron density for the L_D, L_E, and L_F loops compared with the Aβ-free ABAD crystal structure (Figure 1). This is likely due to the increased mobility of these loops upon Aβ binding, which contributes to the positive entropy change in the ABAD−Aβ association. Favorable interactions in these loops are lost upon Aβ binding, which contributes to the positive ΔH of the ABAD−Aβ interaction. For example, residues E112−Q115 in free ABAD form an α-helical structure, whereas in the ABAD−Aβ complex, they become unstructured. The hydrogen bonds formed in this α-helix are broken subsequent to Aβ binding, contributing to the positive ΔH.

The mechanism of Aβ inhibition of ABAD−NAD interaction is likely through the direct distortion of NAD binding sites in ABAD upon Aβ binding. Recently, the focus of research on Aβ toxicity has shifted to different types of soluble Aβ oligomers (*49*−*53*); however, the precise oligomeric state of Aβ that binds to ABAD has not been established. Binding of high-molecular weight Aβ oligomers or soluble fibrils to ABAD can directly distort the NAD binding pocket and displace NAD from its binding site in ABAD. The second possible mechanism is allosteric in nature because the Aβ binding site (L_D loop) is moderately distanced from the NAD binding site (see Figure 1). Binding of lower-molecular weight Aβ oligomers (such as dimer or trimer) may not displace NAD from its binding pocket directly. The third mechanism of Aβ inhibition of NAD binding may occur as a consequence of the increased mobility of NAD binding pockets. This is consistent with the loss of density for the L_D, L_E, and L_F loops upon Aβ binding.

We also showed that NAD inhibits the ABAD−Aβ interaction. With additional NAD in the running buffer, the binding affinity of the ABAD−Aβ interaction was reduced. It is unlikely that a small molecule such as NAD can displace Aβ directly from ABAD. NAD binding may allosterically hold ABAD in a conformational and/or dynamical state not suitable for Aβ binding, especially for the L_D loop.

In summary, SPR revealed a favorable entropic change ($\Delta S = 300 \pm 30$ J mol^{-1} K^{-1}) which overcomes an unfavorable enthalpy change ($\Delta H = 49 \pm 7$ kJ/mol) in the ABAD−Aβ interaction. Therefore, hydrophobic interactions and changes in protein dynamics are the dominant driving forces of the ABAD−Aβ interaction. This is the first dissection of the entropic and enthalpic contribution to the energetics of a protein−protein interaction involving Aβ. Using SPR and STD, we showed that Aβ binding induces conformational and subsequently functional changes, in the form of loss of NAD, in ABAD. Because NAD is the required cofactor for ABAD enzyme activity, Aβ binding results in a loss of ABAD function. Thus, Aβ-induced conformational change may have a role in the mechanism of Aβ toxicity in Alzheimer's disease.

ACKNOWLEDGMENT

We thank Professor Robert Linhardt and Fuming Zhang for helpful discussions.

REFERENCES

1. Hardy, J., and Selkoe, D. J. (2002) The amyloid hypothesis of Alzheimer's disease: Progress and problems on the road to therapeutics, *Science 297*, 353−356.
2. Selkoe, D. J., and Schenk, D. (2003) Alzheimer's disease: Molecular understanding predicts amyloid-based therapeutics, *Annu. Rev. Pharmacol. Toxicol. 43*, 545−584.
3. Small, D. H., Mok, S. S., and Bornstein, J. C. (2001) Alzheimer's disease and Aβ toxicity: From top to bottom, *Nat. Rev. Neurosci. 2*, 595−598.
4. Lustbader, J. W., Cirilli, M., Lin, C., Xu, H. W., Takuma, K., Wang, N., Caspersen, C., Chen, X., Pollak, S., Chaney, M., Trinchese, F., Liu, S., Gunn-Moore, F., Lue, L. F., Walker, D. G., Kuppusamy, P., Zewier, Z. L., Arancio, O., Stern, D., Yan, S. S., and Wu, H. (2004) ABAD directly links Aβ to mitochondrial toxicity in Alzheimer's disease, *Science 304*, 448−452.
5. Yan, S. D., Zhu, Y., Stern, E. D., Hwang, Y. C., Hori, O., Ogawa, S., Frosch, M. P., Connolly, E. S., Jr., McTaggert, R., Pinsky, D. J., Clarke, S., Stern, D. M., and Ramasamy, R. (2000) Amyloid β-peptide-binding alcohol dehydrogenase is a component of the cellular response to nutritional stress, *J. Biol. Chem. 275*, 27100−27109.
6. He, X. Y., Merz, G., Mehta, P., Schulz, H., and Yang, S. Y. (1999) Human brain short chain L-3-hydroxyacyl coenzyme A dehydrogenase is a single-domain multifunctional enzyme. Characterization of a novel 17β-hydroxysteroid dehydrogenase, *J. Biol. Chem. 274*, 15014−15019.
7. He, X. Y., Schulz, H., and Yang, S. Y. (1998) A human brain L-3-hydroxyacyl-coenzyme A dehydrogenase is identical to an amyloid β-peptide-binding protein involved in Alzheimer's disease, *J. Biol. Chem. 273*, 10741−10746.
8. Powell, A. J., Read, J. A., Banfield, M. J., Gunn-Moore, F., Yan, S. D., Lustbader, J., Stern, A. R., Stern, D. M., and Brady, R. L. (2000) Recognition of structurally diverse substrates by type II 3-hydroxyacyl-CoA dehydrogenase (HADH II)/amyloid-β binding alcohol dehydrogenase (ABAD), *J. Mol. Biol. 303*, 311−327.
9. Yan, S. D., Fu, J., Soto, C., Chen, X., Zhu, H., Al-Mohanna, F., Collison, K., Zhu, A., Stern, E., Saido, T., Tohyama, M., Ogawa, S., Roher, A., and Stern, D. (1997) An intracellular protein that binds amyloid-β peptide and mediates neurotoxicity in Alzheimer's disease, *Nature 389*, 689−695.
10. Yan, S. D., Shi, Y., Zhu, A., Fu, J., Zhu, H., Zhu, Y., Gibson, L., Stern, E., Collison, K., Al-Mohanna, F., Ogawa, S., Roher, A., Clarke, S. G., and Stern, D. M. (1999) Role of ERAB/L-3-hydroxyacyl-coenzyme A dehydrogenase type II activity in Aβ-induced cytotoxicity, *J. Biol. Chem. 274*, 2145−2156.
11. Ofman, R., Ruiter, J. P., Feenstra, M., Duran, M., Poll-The, B. T., Zschocke, J., Ensenauer, R., Lehnert, W., Sass, J. O., Sperl, W., and Wanders, R. J. (2003) 2-Methyl-3-hydroxybutyryl-CoA dehydrogenase deficiency is caused by mutations in the HADH2 gene, *Am. J. Hum. Genet. 72*, 1300−1307.
12. Tieu, K., Perier, C., Vila, M., Caspersen, C., Zhang, H. P., Teismann, P., Jackson-Lewis, V., Stern, D. M., Yan, S. D., and Przedborski, S. (2004) L-3-Hydroxyacyl-CoA dehydrogenase II protects in a model of Parkinson's disease, *Ann. Neurol. 56*, 51−60.
13. Torroja, L., Ortuno-Sahagun, D., Ferrus, A., Hammerle, B., and Barbas, J. A. (1998) *scully*, an essential gene of *Drosophila*, is homologous to mammalian mitochondrial type II L-3-hydroxyacyl-CoA dehydrogenase/amyloid-β peptide-binding protein, *J. Cell Biol. 141*, 1009−1017.
14. Sass, J. O., Forstner, R., and Sperl, W. (2004) 2-Methyl-3-hydroxybutyryl-CoA dehydrogenase deficiency: Impaired catabolism of isoleucine presenting as neurodegenerative disease, *Brain Dev. 26*, 12−14.
15. Zschocke, J., Ruiter, J. P., Brand, J., Lindner, M., Hoffmann, G. F., Wanders, R. J., and Mayatepek, E. (2000) Progressive infantile neurodegeneration caused by 2-methyl-3-hydroxybutyryl-CoA dehydrogenase deficiency: A novel inborn error of branched-chain fatty acid and isoleucine metabolism, *Pediatr. Res. 48*, 852−855.

16. Yan, S. D., and Stern, D. M. (2005) Mitochondrial dysfunction and Alzheimer's disease: Role of amyloid-β peptide alcohol dehydrogenase (ABAD), *Int. J. Exp. Pathol. 86*, 161−171.
17. Caspersen, C., Wang, N., Yao, J., Sosunov, A., Chen, X., Lustbader, J. W., Xu, H. W., Stern, D., McKhann, G., and Yan, S. D. (2005) Mitochondrial Aβ: A potential focal point for neuronal metabolic dysfunction in Alzheimer's disease, *FASEB J. 19*, 2040−2041.
18. Anandatheerthavarada, H. K., Biswas, G., Robin, M. A., and Avadhani, N. G. (2003) Mitochondrial targeting and a novel transmembrane arrest of Alzheimer's amyloid precursor protein impairs mitochondrial function in neuronal cells, *J. Cell Biol. 161*, 41−54.
19. Hansson, C. A., Frykman, S., Farmery, M. R., Tjernberg, L. O., Nilsberth, C., Pursglove, S. E., Ito, A., Winblad, B., Cowburn, R. F., Thyberg, J., and Ankarcrona, M. (2004) Nicastrin, presenilin, APH-1, and PEN-2 form active γ-secretase complexes in mitochondria, *J. Biol. Chem. 279*, 51654−51660.
20. Takuma, K., Yao, J., Huang, J., Xu, H., Chen, X., Luddy, J., Trillat, A. C., Stern, D. M., Arancio, O., and Yan, S. S. (2005) ABAD enhances Aβ-induced cell stress via mitochondrial dysfunction, *FASEB J. 19*, 597−598.
21. Munguia, M. E., Govezensky, T., Martinez, R., Manoutcharian, K., and Gevorkian, G. (2006) Identification of amyloid-β 1−42 binding protein fragments by screening of a human brain cDNA library, *Neurosci. Lett. 397*, 79−82.
22. Eckert, A., Keil, U., Marques, C. A., Bonert, A., Frey, C., Schussel, K., and Muller, W. E. (2003) Mitochondrial dysfunction, apoptotic cell death, and Alzheimer's disease, *Biochem. Pharmacol. 66*, 1627−1634.
23. Moreira, P. I., Honda, K., Liu, Q., Santos, M. S., Oliveira, C. R., Aliev, G., Nunomura, A., Zhu, X., Smith, M. A., and Perry, G. (2005) Oxidative stress: The old enemy in Alzheimer's disease pathophysiology, *Curr. Alzheimer Res. 2*, 403−408.
24. Kissinger, C. R., Rejto, P. A., Pelletier, L. A., Thomson, J. A., Showalter, R. E., Abreo, M. A., Agree, C. S., Margosiak, S., Meng, J. J., Aust, R. M., Vanderpool, D., Li, B., Tempczyk-Russell, A., and Villafranca, J. E. (2004) Crystal structure of human ABAD/HSD10 with a bound inhibitor: Implications for design of Alzheimer's disease therapeutics, *J. Mol. Biol. 342*, 943−952.
25. Aguilar, M. I., and Small, D. H. (2005) Surface plasmon resonance for the analysis of β-amyloid interactions and fibril formation in Alzheimer's disease research, *Neurotoxic. Res. 7*, 17−27.
26. Cairo, C. W., Strzelec, A., Murphy, R. M., and Kiessling, L. L. (2002) Affinity-based inhibition of β-amyloid toxicity, *Biochemistry 41*, 8620−8629.
27. O'Shannessy, D. J., Brigham-Burke, M., and Peck, K. (1992) Immobilization chemistries suitable for use in the BIAcore surface plasmon resonance detector, *Anal. Biochem. 205*, 132−136.
28. Karlsson, R., Roos, H., Fagerstam, L., and Persson, B. (1994) Kinetic and concentration analysis using BIA technology, *Methods 6*, 99−110.
29. Day, Y. S., Baird, C. L., Rich, R. L., and Myszka, D. G. (2002) Direct comparison of binding equilibrium, thermodynamic, and rate constants determined by surface- and solution-based biophysical methods, *Protein Sci. 11*, 1017−1025.
30. Myszka, D. G., Abdiche, Y. N., Arisaka, F., Byron, O., Eisenstein, E., Hensley, P., Thomson, J. A., Lombardo, C. R., Schwarz, F., Stafford, W., and Doyle, M. L. (2003) The ABRF-MIRG'02 study: Assembly state, thermodynamic, and kinetic analysis of an enzyme/inhibitor interaction, *J. Biomol. Technol. 14*, 247−269.
31. Hou, L., Shao, H., Zhang, Y., Li, H., Menon, N. K., Neuhaus, E. B., Brewer, J. M., Byeon, I. J., Ray, D. G., Vitek, M. P., Iwashita, T., Makula, R. A., Przybyla, A. B., and Zagorski, M. G. (2004) Solution NMR studies of the Aβ(1−40) and Aβ(1−42) peptides establish that the Met35 oxidation state affects the mechanism of amyloid formation, *J. Am. Chem. Soc. 126*, 1992−2005.
32. Kayed, R., Head, E., Thompson, J. L., McIntire, T. M., Milton, S. C., Cotman, C. W., and Glabe, C. G. (2003) Common structure of soluble amyloid oligomers implies common mechanism of pathogenesis, *Science 300*, 486−489.
33. Hu, W. P., Chang, G. L., Chen, S. J., and Kuo, Y. M. (2006) Kinetic analysis of β-amyloid peptide aggregation induced by metal ions based on surface plasmon resonance biosensing, *J. Neurosci. Methods 154*, 190−197.
34. Liu, R., Yuan, B., Emadi, S., Zameer, A., Schulz, P., McAllister, C., Lyubchenko, Y., Goud, G., and Sierks, M. R. (2004) Single chain variable fragments against β-amyloid (Aβ) can inhibit Aβ aggregation and prevent Aβ-induced neurotoxicity, *Biochemistry 43*, 6959−6967.
35. Inaba, S., Okada, T., Konakahara, T., and Kodaka, M. (2005) Specific binding of amyloid-β-protein to IMR-32 neuroblastoma cell membrane, *J. Pept. Res. 65*, 485−490.
36. Mayer, M., and Meyer, B. (2001) Group epitope mapping by saturation transfer difference NMR to identify segments of a ligand in direct contact with a protein receptor, *J. Am. Chem. Soc. 123*, 6108−6117.
37. Wang, Y. S., Liu, D., and Wyss, D. F. (2004) Competition STD NMR for the detection of high-affinity ligands and NMR-based screening, *Magn. Reson. Chem. 42*, 485−489.
38. Karlsson, R., and Falt, A. (1997) Experimental design for kinetic analysis of protein-protein interactions with surface plasmon resonance biosensors, *J. Immunol. Methods 200*, 121−133.
39. Munoz, E., Xu, D., Kemp, M., Zhang, F., Liu, J., and Linhardt, R. J. (2006) Affinity, kinetic, and structural study of the interaction of 3-O-sulfotransferase isoform 1 with heparan sulfate, *Biochemistry 45*, 5122−5128.
40. Myszka, D. G., Wood, S. J., and Biere, A. L. (1999) Analysis of fibril elongation using surface plasmon resonance biosensors, *Methods Enzymol. 309*, 386−402.
41. de Mol, N. J., Dekker, F. J., Broutin, I., Fischer, M. J., and Liskamp, R. M. (2005) Surface plasmon resonance thermodynamic and kinetic analysis as a strategic tool in drug design. Distinct ways for phosphopeptides to plug into Src- and Grb2 SH2 domains, *J. Med. Chem. 48*, 753−763.
42. Mehta, P. D., Pirttila, T., Mehta, S. P., Sersen, E. A., Aisen, P. S., and Wisniewski, H. M. (2000) Plasma and cerebrospinal fluid levels of amyloid β proteins 1−40 and 1−42 in Alzheimer disease, *Arch. Neurol. 57*, 100−105.
43. Hirai, K., Aliev, G., Nunomura, A., Fujioka, H., Russell, R. L., Atwood, C. S., Johnson, A. B., Kress, Y., Vinters, H. V., Tabaton, M., Shimohama, S., Cash, A. D., Siedlak, S. L., Harris, P. L., Jones, P. K., Petersen, R. B., Perry, G., and Smith, M. A. (2001) Mitochondrial abnormalities in Alzheimer's disease, *J. Neurosci. 21*, 3017−3023.
44. Swerdlow, R. H., and Khan, S. M. (2004) A "mitochondrial cascade hypothesis" for sporadic Alzheimer's disease, *Med. Hypotheses 63*, 8−20.
45. Manczak, M., Park, B. S., Jung, Y., and Reddy, P. H. (2004) Differential expression of oxidative phosphorylation genes in patients with Alzheimer's disease: Implications for early mitochondrial dysfunction and oxidative damage, *Neuromol. Med. 5*, 147−162.
46. Nunomura, A., Perry, G., Aliev, G., Hirai, K., Takeda, A., Balraj, E. K., Jones, P. K., Ghanbari, H., Wataya, T., Shimohama, S., Chiba, S., Atwood, C. S., Petersen, R. B., and Smith, M. A. (2001) Oxidative damage is the earliest event in Alzheimer disease, *J. Neuropathol. Exp. Neurol. 60*, 759−767.
47. Cardoso, S. M., Santos, S., Swerdlow, R. H., and Oliveira, C. R. (2001) Functional mitochondria are required for amyloid β-mediated neurotoxicity, *FASEB J. 15*, 1439−1441.
48. Yan, Y., and Wang, C. (2006) Aβ42 is More Rigid than Aβ40 at the C Terminus: Implications for Aβ Aggregation and Toxicity, *J. Mol. Biol. 364*, 853−862.
49. Klein, W. L. (2002) Aβ toxicity in Alzheimer's disease: Globular oligomers (ADDLs) as new vaccine and drug targets, *Neurochem. Int. 41*, 345−352.
50. Walsh, D. M., and Selkoe, D. J. (2004) Oligomers on the brain: The emerging role of soluble protein aggregates in neurodegeneration, *Protein Pept. Lett. 11*, 213−228.
51. Walsh, D. M., Klyubin, I., Shankar, G. M., Townsend, M., Fadeeva, J. V., Betts, V., Podlisny, M. B., Cleary, J. P., Ashe, K. H., Rowan, M. J., and Selkoe, D. J. (2005) The role of cell-derived oligomers of Aβ in Alzheimer's disease and avenues for therapeutic intervention, *Biochem. Soc. Trans. 33*, 1087−1090.
52. Walsh, D. M., Klyubin, I., Fadeeva, J. V., Rowan, M. J., and Selkoe, D. J. (2002) Amyloid-β oligomers: Their production, toxicity and therapeutic inhibition, *Biochem. Soc. Trans. 30*, 552−557.
53. Lue, L. F., Kuo, Y. M., Roher, A. E., Brachova, L., Shen, Y., Sue, L., Beach, T., Kurth, J. H., Rydel, R. E., and Rogers, J. (1999) Soluble amyloid β peptide concentration as a predictor of synaptic change in Alzheimer's disease, *Am. J. Pathol. 155*, 853−862.

BI061314N